

Comparison of the static and dynamic modulus of rock mass determined by seismic measurements

Krzysztof Krawiec

k.krawiec@meeri.pl |  <https://orcid.org/0000-0002-5765-1387>

Zenon Pilecki

pilecki@meeri.pl |  <https://orcid.org/0000-0002-0090-8743>

Mineral and Energy Economy Research Institute of the Polish Academy of Sciences, Poland

Piotr Koziot

piotrkoz@oslomet.no |  <https://orcid.org/0000-0001-9685-1923>

Oslo Metropolitan University, Norway

Scientific Editor: Andrzej Winnicki,
Cracow University of Technology

Technical Editor: Aleksandra Urzędowska,
Cracow University of Technology Press

Typesetting: Małgorzata Murat-Drożyńska,
Cracow University of Technology Press

Received: October 24, 2025

Accepted: November 29, 2025

Copyright: © 2025 Krawiec, Pilecki, Koziot. This is an open access article distributed under the terms of the Creative Commons Attribution License, which permits unrestricted use, distribution, and reproduction in any medium, provided the original author and source are credited.

Data Availability Statement: All relevant data are within the paper and its Supporting Information files.

Competing interests: The authors have declared that no competing interests exist.

Citation: Krawiec, K., Pilecki, Z., Koziot, P. (2025). Comparison of the static and dynamic modulus of rock mass determined by seismic measurements. *Technical Transactions*, e2025018. <https://doi.org/10.37705/TechTrans/e2025018>

Abstract

The study aimed to compare the quasi-static moduli determined from the empirical Barton relationship with the dynamic modulus of elasticity for various types of rock strata. Both moduli were determined from measured P- and S-wave velocities obtained by seismic refraction profiling or seismic tomography. The moduli were calculated using the Barton relationship, which requires only the P-wave velocity, while the dynamic modulus of elasticity was calculated from the P- and S-wave velocities and the bulk density of rock material. The study was conducted on various rock masses, ranging from weak, highly fractured, weathered rock to very strong rock, at different depths in Poland. The study revealed that the dynamic modulus of elasticity is significantly higher than the quasi-static deformation moduli. The relative difference between the moduli ranges from 13 to 54%. In rocks more heavily fractured by weathering and anthropogenic activity, the difference in moduli was greatest, ranging from 44 to 54%. For other rocks with less weathering and not disturbed, the relative difference ranged from 13 to 20%. More severe fractures, resulting from both weathering and anthropogenic activity, result in greater discrepancies in modulus calculations. These findings provide more effective insights into the applications of seismic-determined moduli in geotechnical problems.

Keywords: static deformation modulus, dynamic modulus of elasticity, seismic method, P- and S-wave velocities

1. Introduction

The deformation modulus of a rock mass is a key parameter in geotechnics, used to estimate the behaviour of the bedrock of building structures and the rock mass around underground structures such as tunnels and mine workings (Bieniawski, 1989; Hoek et al., 1995; Kudyk and Pilecki, 2009; Tajduś et al., 2012; Majcherczyk et al., 2012). This parameter describes the stiffness of the rock mass, i.e., its ability to deform under the influence of various types of loads. It is an important input parameter for numerical modelling of rock mass behaviour (Hoek et al., 1995; Pilecki, 1999; Barton, 2007; Pilecki et al., 2025).

The static deformation modulus of a rock mass is lower compared to the modulus of the rock material determined in laboratory tests. This is because the stiffness of a rock mass is usually reduced by various types of discontinuities, primarily fractures and, sometimes, waterlogging. Barton (2006) reports that the deformation modulus of a rock mass, in terms of elastic and inelastic behaviour, usually lies between 0.1 and 100 GPa. Discontinuities in a rock mass, and especially their number, orientation, and characteristics, such as the filling of cracks with clay material, significantly reduce the stiffness of the mass and thus the deformation modulus. However, a rock sample is approximately homogeneous and undisturbed by fractures that would cause its instability.

The deformation modulus of a rock mass may depend on the size of the rock volume being tested. Measurements on small volumes can yield significantly higher values than those on large volumes, as the latter include extensive fracture zones. It should also be emphasised that as the depth of the tested rock mass increases, and thus the gravitational stress increases, the deformation modulus may increase due to pore compression and the closure of fractures.

The deformation modulus of a rock mass can be measured using direct or indirect methods. In indirect methods, the deformation modulus is determined primarily from correlations with geotechnical classification punctuation for rock masses. Correlation with the RMR (Rock Mass Rating) system, as developed by Bieniawski (1989), is commonly used. Correlations with the Q geotechnical system (Barton et al., 1974) or the Geological Strength Index (GSI) system by Hoek and Brown (1980) are well established.

Direct methods primarily include dilatometric tests, plate loading tests, and the seismic method. Dilatometric and plate-loading tests reflect the complete response of the rock mass to loading, as they account for both elastic and inelastic deformations. Tests are performed under quasi-static conditions, where a load is applied continuously and slowly.

Typically, the plate-bearing test has been the most commonly used (Barton, 2007). Plate measurements involve loading the rock surface using hydraulic rams and require careful preparation of the ground surface. A significant advantage of borehole dilatometer measurements is that they enable the determination of the deformation moduli of rock layers at various depths. A limitation is the range of the dilatometer. There are other small-scale types of in-situ tests, such as borehole jacking tests. In general, borehole tests may yield higher moduli than plate-bearing tests because they involve smaller volumes of rock mass (Barton, 2006).

The seismic method can determine the dynamic Young's modulus of elasticity or the quasi-static deformation modulus based on empirical correlations with seismic parameters. The seismic method for determining the modulus of a rock mass involves measuring various seismic parameters, such as the propagation velocities of P- and S-wave and the wave frequency. Measurements are most often performed using refraction profiling or tomography, and in the case of an accessible borehole, using various borehole techniques (Barton, 2006; Pilecki, 2018).

The dynamic modulus of elasticity is determined from the measured propagation velocities of longitudinal P and transverse S seismic waves in the rock mass. It is assumed that the stiffness of a rock mass is determined over a very small range of elastic deformations. The dynamic modulus of elasticity can be determined in the laboratory on rock samples by measuring the



propagation velocity of P- and S-waves. The modulus of elasticity determined in the laboratory for the rock sample yields higher values because it does not account for the effect of discontinuities within the rock mass. The quasi-static deformation modulus can be determined from correlation relationships with seismic parameters. Most often, the deformation modulus can be determined from the empirical relationship proposed by Barton (2006), which is based on the P-wave velocity and developed using the geotechnical classification Q_c score. This issue is discussed in more detail in Section 2.2. The deformation modulus can also be estimated from an empirical relationship that accounts for S-wave frequency (Bieniawski, 1978). The test methodology in this case utilises the “petite seismique” technique proposed by Schneider (1967).

The dynamic modulus of elasticity of a rock mass determined by seismic methods assumes higher values than the modulus determined by traditional static methods (dilatometric tests or plate-loading tests). Numerous examples of correlations between dynamic and static moduli are known, such as those reported by Ide (1936), Linowski (1969), and Sjögren et al. (1979).

The purpose of this study is to compare the quasi-static moduli determined from Barton's (2006) relationship with the dynamic modulus of elasticity for various types of rock masses. Modulus calculations were performed using the same measured data; Barton's formulae require only knowledge of the P-wave velocity, whereas the dynamic modulus of elasticity was calculated from the P-wave velocity, S-wave velocity, and bulk density. The studies were conducted using either seismic refraction profiling or seismic tomography. The study examined modulus values for an exceptionally fractured limestone mass subjected to long-term weathering processes and the impact of explosive mining. This article discusses the limitations of the seismic method for determining rock modulus. The assumptions of Barton's empirical equation are described. The results of dynamic and quasi-static modulus calculations for rock layers of varying quality at various depths are compared. The analysis assessed the usefulness of seismic studies for determining rock modulus and their application in geotechnical problems.

2. Methods and materials

2.1. Limitations of the seismic method in determining the mechanical parameters of a rock mass

In seismic surveys, many factors significantly influence the determined seismic parameters of rocks (Anderson et al., 1974; Barton, 2006; Pilecki, 2018). These factors are related to the physical characteristics of the rock mass:

- ▶ Primary: such as the mineral composition of the rock, structural elements related to the rock formation process, such as layering, joints and tectonic fractures, the state of stress and deformation, and the temperature of the rock mass resulting from the depth of occurrence.
- ▶ Secondary: acquired under the conditions of occurrence as a result of weathering processes and various anthropogenic activities, such as mining with machinery and explosives, construction activities, the impact of various vibrations, etc.

When determining the mechanical parameters of a rock mass using seismic methods, a section with limited influence from secondary characteristics should be selected. In layered media, the rock's anisotropy influences the measured refractive wave velocities. However, fractures are among the most critical factors affecting the elastic properties of a rock mass.

Based on the knowledge of the longitudinal wave velocity V_p , shear wave velocity V_s , and bulk density ρ , the dynamic Young's modulus of elasticity E_d is calculated:

$$E_d = \rho (V_s)^2 \frac{\frac{3(V_p)^2}{V_s} - 4}{\left(\frac{V_p}{V_s}\right)^2 - 1} \quad (1)$$

Relationship (1) denotes that changes in the velocity of P- and S-waves indicate changes in the elastic properties of the rock mass. Numerous studies demonstrate that such changes may indicate the influence of weak zones, especially fractures and voids (Dubiński and Konopko, 2000; Marcak and Zuberek, 1994; Pilecki et al., 2013; Łapczyński et al., 2025). It is also important to emphasise the difficulties in determining the S-wave velocity. While the identification of P-wave onset is evident in most cases, S-wave onset requires various procedures during measurement and data processing (Reynolds, 2011; Harba et al., 2017, 2019; Pilecki, 2018). Knowledge of the dynamic modulus of elasticity E_d and the dynamic Poisson's ratio ν_d allows for the calculation of the shear modulus $G_d = E_d / 2(1+\nu_d)$ and the bulk modulus $K_d = E_d / 3(1-2\nu_d)$. The dynamic shear modulus is often determined directly from 1D S-wave velocity profiling (Pilecki, 2018). Using the seismic method for this purpose allows avoiding the limitations associated with sampling and the influence of local inhomogeneities on the results obtained with typical geotechnical methods. Furthermore, in weak rocks, the stress-strain relationship is nonlinear even at very small strains (Reynolds, 2011). Therefore, seismic methods based on small strain allow the determination of the maximum stiffness of elastic rock behaviour. For strains less than 0.001%, i.e., in the seismic range, stiffness is greatest. In the rock strain range (0.001–0.1%), stiffness is directly proportional to strain; however, at large strains (>0.01%), the rock exhibits plastic behaviour (Reynolds, 2011). The development of a fracture in the rock mass causes the strain to increase. Consequently, the stiffness of the rock mass decreases. Therefore, the value of the deformation modulus of deteriorated rock mass will be smaller than the value of the dynamic elastic modulus.

2.2. Relationship between deformation modulus Em, Qc classification and P-wave velocity

The Q_c classification (Barton, 2006) is a modification of the well-known geotechnical Q classification (Barton et al., 1974), which uses the P-wave velocity to determine the deformation modulus of the rock mass. The classification was developed based on the results of seismic refraction and cross-hole tomography studies. Barton (1996, 2006) modified the Q system by introducing the uniaxial strength σ_c of the rock material, so that:

$$Q_c = Q \frac{\sigma_c}{100} \quad (2)$$

This modification was intended to achieve a more favourable correlation of the deformation modulus E_m with the seismic velocity V_p . The result was a normalised score that reduces or increases the Q score for rock masses weaker or stronger than 100 MPa, respectively. Based on the analysis of the P-wave velocity V_p and the Q_c score, which took into account the data of Sjögren et al. (1979), he developed the following relationship:

$$V_p = \log Q + 3.5 \left[\frac{km}{s} \right] \quad (3)$$

However, after taking into account the empirical dependence of the quasi-static deformation modulus E_m on the Q_c score (Barton 1995, 2006) in the form:

$$E_m \approx 10 \cdot Q_c^{\frac{1}{3}} \text{ and} \quad (4)$$

$$Q_c = Q \cdot \frac{\sigma_c}{100} \quad (5)$$

the following relationship was obtained, which allows for determining this modulus as a function of velocity V_p :

$$E_m \approx 10 \cdot 10^{\frac{(V_p - 3.5)}{3.0}} \quad (6)$$

where the velocity V_p is in [km/s].

The determined modulus E_m is an average value resulting from the seismic measurement methodology. The modulus values for the zone of strong fracture of the rock mass are described by the formula (Barton, 1996):

$$E_{m_{\min}} \approx 3Q_c^{1/3} \quad (7)$$

Barton (1996, 2006) developed a Q_c classification nomogram that includes depth and porosity as key factors affecting seismic wave velocity (Fig. 1). This nomogram is based on data from sites with softer rocks, such as chalk, chalk marl, sandstones, shales, and some weathered volcanic, igneous, and metamorphic rocks, where both seismic velocities and core-logged Q -values were available. Extensive data were collected from tunnelling and cavern projects in England, Norway, Israel, Hong Kong, and China (Barton, 2007). The bold diagonal line in the nomogram is derived from the average of hard rock and shallow seismic refraction data (diagonal line), partly based on the study by Sjögren et al. (1979). This line applies specifically to low-porosity rocks at a depth of approximately 25 meters. The straight lines above the bold line represent velocity and rock quality relationships applicable at greater depths, while the straight lines below the bold line provide approximate corrections for higher porosity rocks.

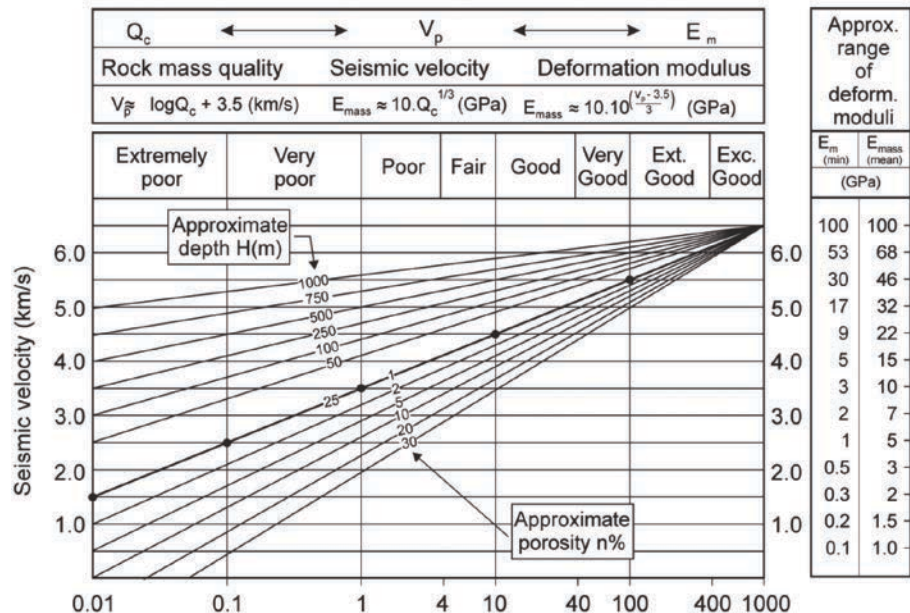


Fig. 1. Nomogram for determining the quasi-static deformation modulus of a rock mass (Barton, 2006)

$$Q_c = \left[\frac{RQD}{J_n} \times \frac{J_r}{J_a} \times \frac{J_w}{SRF} \right] \frac{\sigma_c}{100}$$

The mean rock mass deformation modulus values, shown on the right side of Figure 1, were derived from case histories. These relationships were obtained from plate-bearing tests or from analyses of tunnel and shaft deformation. In the latter, multiple-position borehole extensometers may be used to obtain depth-dependent moduli in the excavation-damaged zone, or a simple convergence

measurement can be used to back-calculate approximate estimates of E_m . The low values of $E_{m(\min)}$, also included in the table, are attributed to loosening in the excavation-disturbed zone that typically surrounds test sites and tunnel excavations in rock (Barton, 2007).

Barton (2007) introduced the seismic quality factor for P-waves (Q_p), which shows a strong correlation with the rock mass quality factor (Q). In general, lower values of Q_p are found in weathered or fractured zones, while higher values are observed in compact rock masses. Within the first kilometre of jointed rock, Q_p displays a remarkable similarity to the deformability modulus (E_m). He modified relation 5 with knowledge of the uniaxial strength σ_c of rock material in the form:

$$E_{m(\min)} \approx Q_p \approx 10^{(V_p - 2.5 + \log \sigma_c)/3} \quad (8)$$

Dependence (8) may be used to estimate E_m or Q_p from measurements of V_p and σ_c for rock masses in the near-surface (Barton, 2007). Relating E_m to V_p and uniaxial strength σ_c , Barton (2007) introduced a nomogram presented in Figure 2. He considered it reasonable to apply equation (8) of saturated jointed crust, beyond which the empirical database for moduli measurements declines sharply.

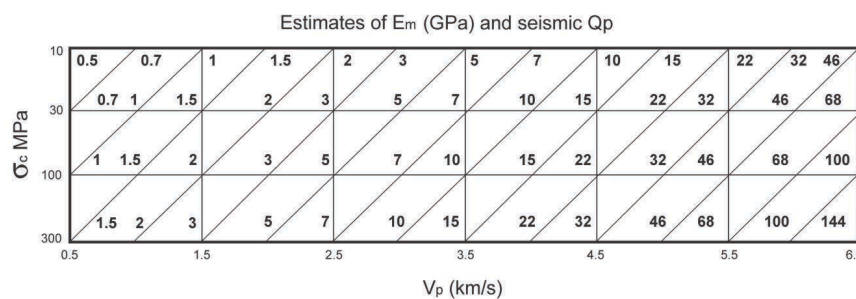


Fig. 2. Nomogram relating E_m to V_p and uniaxial strength σ_c (Barton, 2007)

2.3. Geological data

P- and S-wave velocity measurements were obtained in various rock layers at different depths as part of engineering seismic surveys conducted in Poland over the past decade. Measurements were taken at the ground surface and in an underground mine at approximately 1,000 m depth. Seismic data were measured in the following rock layers:

- ▶ Limestone (Lower and Middle Cambrian): dark grey, slightly metamorphosed, unevenly layered, and highly fractured due to intense weathering and the impact of explosive mining. The top of the studied layer was located at approximately 2 m depth.
- ▶ Weathered limestone (Lower and Middle Cambrian): dark grey, with a higher density of fractures intensified by weathering processes. The studied layer was located in the subsurface zone to a depth of approximately 2 m.
- ▶ Calcareous marls (Upper Cretaceous – Turonian): light grey with a high calcium carbonate content, plate-like, thick-bedded, horizontally bedded, with bedding becoming less pronounced with depth, highly fractured, and with numerous fracture systems. The fracture systems were deepened by weathering processes, which disappear deeper into the rock massif (Alexandrowicz and Radwan, 1973). The top of the studied layer is approximately 3 m deep.
- ▶ Lower marls (Upper Cretaceous – Turonian): light grey and grey, horizontally bedded, highly fractured, with distinct joints, and with sparse tectonic fractures, with a thickness ranging from 12 to 17 m (Alexandrowicz and Radwan, 1973). The top of the studied layer is approximately 10 m deep.

- ▶ Clay marls (Upper Cretaceous - Turonian): grey and dark grey with a high clay content, less intense fractures. Fractures cause the rock to form roughly regular blocks; tectonic fractures are rare, and the thickness ranges from 8 to 12 m (Alexandrowicz and Radwan, 1973). The top of the studied layer lies at approximately 26 m.
- ▶ Sandstones (Upper Cretaceous - Cenomanian): grey and greenish-grey, fine-grained and silty with intercalations of medium-grained sands, poorly cemented, the cement is marly, and the bedding is indistinct, reaching a thickness of 4 to 8 m (Alexandrowicz and Radwan, 1973). The top of the studied layer lies at approximately 35 m depth.
- ▶ Calcareous dolomite (Permian-Zechstein): grey, with distinct plate discontinuity, bedded from 0.1 to 0.6 m, total thickness up to approximately 9 m. Irregular zones of higher porosity, fractures, and occasional water presence occur (Peryt, 1978; Ślizowski et al., 2013). The top of the studied layer lies at approximately 1000 m depth.
- ▶ Granite (Carboniferous): grey, often with a distinct greenish tinge, fine-to medium-grained, highly compact, poorly weathered, characterised by a distinct joint in three perpendicular directions. The top of the studied layer lies at approximately 50 m depth.

3. Results and analysis

3.1. Example of modulus determination in an intensely fractured Cambrian limestone rock mass using refraction profiling

Experimental studies were conducted on an intensively fractured Cambrian limestone massif subjected to the effects of explosive mining and long-term weathering. A seismic refraction profile was performed on a rock shelf excavated several decades ago in a quarry in the Sudetes. The study aimed to compare the quasi-static modulus of deformation, as defined by Barton's formula (6), with the dynamic modulus of elasticity (1) for an intensively fractured rock mass. A schematic of the seismic refraction profile is presented in Figure 3.

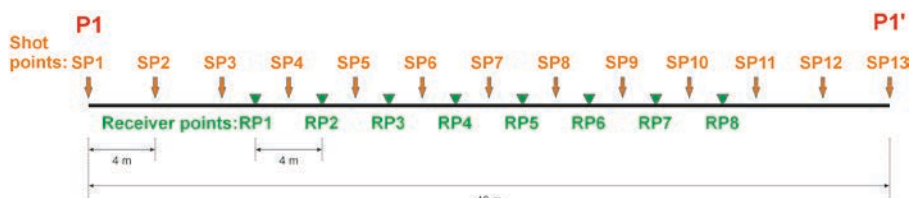


Fig. 3. Schematic of refraction seismic profiling in the limestone layer (own elaboration)

Seismic measurements were conducted along a 28-meter-long profile with geophones installed every 4 meters. Wave excitation points were also located every 4 meters between the geophones. Eight three-component 4,5 Hz GS-11D geophones, manufactured by Geospace, were utilised for the measurements. The sensors were positioned to measure waves in three directions: vertically (y-axis) and horizontally in the x1 direction (parallel to the profile) and the x2 direction (perpendicular to the profile).

The wave was generated by striking a metal plate with a 4-kg sledgehammer, which was stacked eight times. Data collection was performed using a Geode 24-channel instrument produced by Geometrics. Seismic data processing and interpretation were carried out using the Pickwin and Seisimager software, both from Geometrics. The interpretation was performed using a classical refraction algorithm.

The modulus calculation results are summarised in Table 1. Comparison of the moduli shows that the dynamic modulus of elasticity for both layers is approximately twice the Barton deformation modulus. The primary reason for the difference in the two modulus values is the degree of rock fracture,

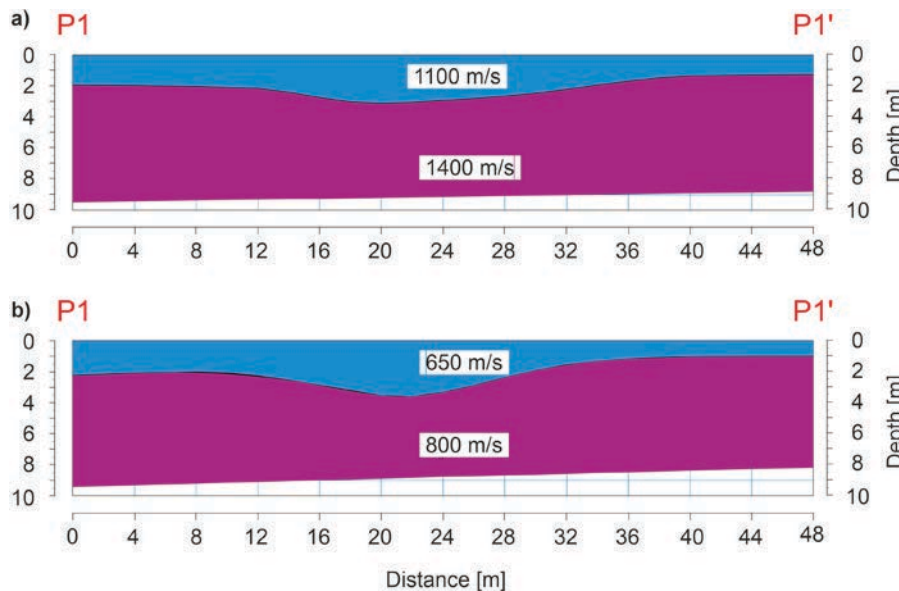


Fig. 4. Seismic model for P-wave (a) and S-wave (b) velocity in the limestone rock mass (own elaboration)

which is intensified in the near-surface zone. This indicates that fractures have a significant impact on modulus calculations. It should be emphasised that the measured velocities in both layers are relatively low. In the case of a compact limestone rock mass, unweathered and undisturbed by the action of explosives, the P wave velocity should be approximately 4,000 m/s. Such a significant decrease in velocity to approximately 1,400 m/s in layer II of the seismic model may indicate that rock fractures were quite intensively developed.

Table 1. Dynamic elastic modulus and deformation modulus for the limestone rock mass (own elaboration)

Seismic layer	Mean P-wave velocity [m/s]	Mean S-wave velocity [m/s]	Dynamic elastic modulus E_d [GPa]	Deformation modulus E_m [GPa]
Layer I	1100	650	2.83	1.58
Layer II	1400	800	4.38	2.00

3.2. Comparison of the quasi-static deformation modulus and the dynamic modulus of elasticity determined by the seismic method

It should be emphasised that both mathematical formulas for calculating the quasi-static deformation modulus (6) and the dynamic modulus of elasticity (1) are based on determining the velocity of the P-wave or the P- and S-waves, respectively. The measurement methodology is identical.

Table 2 summarises the measured P-wave velocity ranges and the deformation modulus E_m values calculated using formula (6) for the analysed rock layers. In the case of the near-surface zone, the velocity values varied significantly depending on the degree of rock weathering in this zone.

Table 3 presents the calculated dynamic modulus of elasticity values for the measured P- and S-wave velocities in the corresponding geological layers, with the bulk densities of the rock material assumed as given in Table 4.

Table 4 summarises the mean velocity ratios V_p/V_s and the relative modulus differences expressed as percentages for the analysed rock layers.

The results of the calculations show that Carboniferous granite and Permian dolomite have the largest quasi-static deformation moduli, at 17.78 and 64.57 GPa, respectively (Table 2). Similarly, the dynamic elastic moduli are the largest, at 34.79 and 78.15 GPa, respectively (Table 3). These are strong

Table 2. The quasi-static deformation modulus E_m for different rock layers according to formula (6) (own elaboration)

No.	Geological Layer	Depth ¹ [m]	P-wave velocity V_p [km/s]			Deformation modulus E_m [GPa]		
			Min.	Max.	Mean	Min.	Max.	Mean
1.	Cambrian limestone intensively fractured	approx. 3	-	-	1.4	-	-	2.00
2.	Cambrian limestone (1) subsurface	up to 3	-	-	1.1	-	-	1.58
3.	Carboniferous granite weathered	approx. 50	3.70	4.80	4.25	11.66	27.12	17.78
4.	Upper Cretaceous calcareous marl	approx. 3	0.87	2.10	1.49	1.33	3.41	2.37
5.	Upper Cretaceous lower marl	approx. 10	1.70	2.63	2.17	2.51	5.13	3.82
6.	Upper Cretaceous clayey marl	approx. 26	2.15	3.00	2.58	3.55	6.81	5.18
7.	Upper Cretaceous sandstone	approx. 35	2.84	-	-	6.03	-	>6.03
8.	Permian dolomite	approx. 1000	5.68	6.17	5.93	53.29	77.62	64.57

¹Depth to the top of the lithological layer;

Table 3. Dynamic modulus of elasticity for different rock layers according to formula (1) (own elaboration)

No.	Geological Layer	P-wave velocity V_p [km/s]			S-wave velocity V_s [km/s]			Dynamic elastic modulus [GPa]		
		Min.	Max.	Mean	Min.	Max.	Mean	Min.	Max.	Mean
1.	Cambrian limestone intensively fractured	-	-	1.4	-	-	0.8	-	-	4.38
2.	Cambrian limestone (1) subsurface	-	-	1.1	-	-	0.65	-	-	2.83
3.	Carboniferous granite weathered	3.70	4.80	4.25	1.90	2.56	2.23	25.46	45.54	34.79
4.	Upper Cretaceous calcareous marl	0.87	2.10	1.49	0.63	0.74	0.67	1.70	3.54	2.89
5.	Upper Cretaceous lower marl	1.70	2.63	2.17	0.83	0.89	0.86	3.92	4.81	4.40
6.	Upper Cretaceous clayey marl	2.15	3.00	2.58	0.89	1.17	1.03	4.80	8.38	6.47
7.	Upper Cretaceous sandstone	2.84	-	-	1.00	-	-	7.28	-	>7.28
8.	Permian dolomite	5.68	6.17	5.93	3.17	3.44	3.31	71.68	84.46	78.15

Table 4. Table 4. Relative difference in mean moduli for rock layers (own elaboration)

No.	Geological Layer	Bulk density ¹ ρ [kg/m ³]	Mean V_p [km/s]	Mean V_s [km/s]	Relative difference R ² [%]
1.	Cambrian limestone intensively fractured	2720	1.4	0.80	54
2.	Cambrian limestone (1) subsurface	2720	1.1	0.65	44
3.	Carboniferous granite weathered	2670	4.25	2.23	48
4.	Upper Cretaceous calcareous marl	2150	1.49	0.67	18
5.	Upper Cretaceous lower marl	2140	2.17	0.86	13
6.	Upper Cretaceous clayey marl	2170	2.58	1.03	20
7.	Upper Cretaceous sandstone	2310	2.84 ³	1.00 ³	17
8.	Permian dolomite	2800	5.93	3.31	17

¹Mean bulk density of rock material; ²Relative difference between the moduli $R(\%) = ((E_d E_m) / E_d) \cdot 100\%$; ³Minimal value

rocks, but weathering processes have caused the stiffness of the rock layers to decrease. However, the reduced P- and S-wave velocities in weathered granite result in a relatively significant difference in moduli, amounting to 48% (Table 4). In contrast, for Permian dolomite at a depth of 1000 m, the relative difference in moduli is 17%. This indicates that additional fractures resulting from weathering processes in Carboniferous granite increase the relative difference in moduli. This is particularly evident in the case of Cambrian limestone, which was intensively fractured by explosives during mining, and

further fractures developed over long-term weathering. In this case, we have relatively low values of the deformation modulus $E_m = 2.0$ GPa and the elastic modulus $E^d = 4.38$ GPa, with a relative difference of 54%. Similar moduli are found in weathered Cambrian limestone at a depth of approximately 3.0 m. If we assume a typical P-wave velocity of 4000 m/s for the compact Cambrian limestone rock mass, then the deformation modulus is significantly higher, at 14.8 GPa. The examples presented indicate that the relative differences in the moduli can be approximately 20% if the rock is not subject to excessive fracturing from weathering and other processes, e.g., mining.

This observation is confirmed by modulus calculations for the weaker Turonian rocks in the Upper Cretaceous. All studied marls have similar moduli of deformation, ranging from 2.37 GPa for the calcareous marl, 3.82 GPa for the lower marl, to 5.18 GPa for the clayey marl (Table 2). Higher moduli of elasticity are 2.89, 4.40, and 6.47 GPa, respectively (Table 3). Relative differences between moduli are 18, 13, and 20% (Table 4). In their conditions of occurrence, these rocks were subject to less intense weathering processes with increasing depth. Fracture intensity decreased with depth, as evidenced by the measured P- and S-wave velocities (Table 3). Only slightly higher moduli are observed in the Cenomanian sandstone of the Upper Cretaceous. It occurs directly below the marls; however, studies were conducted only on the upper part of the layer because the adopted refraction profiling methodology was limited to a specific depth range. Therefore, Tables 2 to 4 provide only the minimum values of P- and S-wave velocities and calculated moduli.

Nevertheless, the calculation results are similar to those for marls, with a relative difference of 17%. This also confirms the observations regarding the applicability of both moduli. Our observations on undisturbed or slightly disturbed rocks are consistent with Siggins's (1993) conclusions. He found that dynamic moduli are, on average, about 30% higher than static moduli. Minor differences, e.g., 5-25% for strong rocks, are also reported in the literature (Ide, 1936; Sutherland, 1962). However, in weak rocks, especially those intensely fractured by weathering and other processes, including anthropogenic processes, these differences can be many times greater (e.g., McCann et al., 1990).

However, the comparison of quasi-static moduli from Barton's equation (6) to dynamic elastic moduli (1) determined seismically requires further research on rock masses with different moduli, including at different depths.

4. Conclusions

Based on the research results presented in this article, the following conclusions can be drawn:

- 1) In engineering practice, when designing structures on bedrock or within a rock mass, it is most advantageous to adopt the static deformation modulus determined in situ because it realistically describes the behaviour of the rock under the influence of loads. This method examines the rock mass's response to static loading, which induces significant deformations. However, dilatometric or plate-loading tests are cumbersome and expensive. Therefore, the dynamic modulus of elasticity derived from in situ seismic measurements can be used in calculations.
- 2) The dynamic modulus of elasticity describes the response to short-term, small-scale quasi-elastic deformations of the rock mass induced by the propagation of seismic waves. The stiffness of the medium is measured at a small-strain scale, taking into account the weakening associated with fractures and waterlogging.
- 3) The static modulus of deformation cannot be directly determined using the seismic method. This is due to fundamental differences in the measurement methodology and the physics underlying the phenomena used to determine this modulus. However, it can be determined from empirical correlations



between the quasi-static modulus and seismic parameters, such as those presented in the formulas by Barton (2006) or Bieniawski (1978).

- 4) Rock fractures have a significant impact on the velocities of both P- and S-waves and, consequently, on the calculations of dynamic and quasi-static moduli in the seismic method. In the studies, the relative difference between moduli ranged from 13 to 54%. In more strongly fractured rocks resulting from weathering processes and anthropogenic activity, the difference in moduli was largest between Cambrian limestone and Carboniferous granite, ranging from 44 to 54%. For the remaining compact and less weathered rocks, the relative difference ranged from 13 to 20%. More intense fractures, resulting from both weathering and anthropogenic activity, lead to significant differences in modulus calculations.
- 5) The depth of the rock layers should be taken into account in these calculations. As depth increases, the differences in moduli decrease. This is because, as velocity increases with depth, it results in less weathering, closing joints, less clay, and usually a reduced frequency of jointing (Barton, 2006).
- 6) The seismic method is a valuable tool for approximate estimation of the deformation modulus based on seismic parameters, but it does not replace direct load measurements. The quasi-static modulus of deformation determined using the Barton (2006) equations assumes lower values than the dynamic modulus of elasticity.
- 7) Seismic measurements reflect the mechanical response of the rock mass within the very small strain range, where stiffness is maximal. Under quasi-static load, the fracture processes are mobilised, reducing the effective modulus. The strain-dependent stiffness degradation in intact and fractured rocks is well documented in experimental mechanics (Paterson and Wong, 2005). Thus, the larger divergence observed for modulus values for highly fractured rock layers is justified.

It should be emphasised that isolinear modulus maps are used to identify zones of weakness and strengthening in rock mass. They are used in mining and tunnelling applications.

References

Alexandrowicz, S.W., Radwan, D. (1973). Kreda opolska – problematyka stratygraficzna i złożowa. *Przegląd Geologiczny* 4, 183–188.

Anderson, D.L., Minster, B., & Cole, D. (1974). The effect of oriented cracks on seismic velocities. *Journal of Geophysical Research* 79, 4011–4015.

Barton, N., Lien, R., & Lunde, J. (1974). Engineering classification of rock masses for the design of tunnel support. *Rock Mechanic*, 6(4), 189–239.

Barton, N. (1995). The influence of joint properties in modeling of jointed rock masses. *Keynote lecture presented at the 8th International Society for Rock Mechanics Congress*, Tokyo (Vol. III, pp. 1023–1032). Rotterdam: Balkema.

Barton, N. (1996). Estimating rock mass deformation modulus for excavation disturbed zone studies. In J.B. Martino & C.D. Martin (Eds.), *Proceedings of the Excavation Disturbed Zone Workshop* (pp. 133–144). Manitoba, Canada, September 20, 1996.

Barton, N. (2006). *Rock Quality, Seismic Velocity, Attenuation and Anisotropy*. Taylor & Francis: UK and The Netherlands.

Barton, N. (2007). Near-surface gradients of rock quality, deformation modulus, V_p and Q_p to 1 km depth. *First Break* 25(10), 53–60.

Bieniawski, Z.T. (1978). Determining rock mass deformability: Experience from case histories. *International Journal of Rock Mechanics and Mining Sciences & Geomechanics Abstracts* 15, 237–247.

Bieniawski, Z.T. (1989). *Engineering rock mass classification*. New York: Wiley.

Dubiński, J. Konopko, W. (2000). *Tąpania: ocena, prognoza, zwalczanie*. Katowice: Główny Instytut Górnictwa.

Harba, P., Pilecki, Z. (2017). Assessment of time-spatial changes of shear wave velocities of flysch formation prone to mass movements by seismic interferometry with use of ambient noise. *Landslide* 14(3), 1225–1233. <https://doi.org/10.1007/s10346-016-0779-2>.

Harba, P., Pilecki, Z., Krawiec, K. (2019). Comparison of MASW and seismic interferometry with use of ambient noise for estimation of S-wave velocity field in landslide subsurface. *Acta Geophysica* 67, 1875–1883. <https://doi.org/10.1007/s11600-019-00344-9>.

Hoek, E., Brown, E.T. (1980). *Underground Excavation in Rock*. London: Institution of Mining and Metallurgy.

Hoek, E., Kaiser, P.K., & Bawden, W.F. (1995). *Support of underground excavations in hard rock*. Rotterdam: Balkema.

Ide, J. M. (1936). Comparison of statically and dynamically determined Young's modulus of rocks. *Proceedings of the National Academy of Sciences* 22(2), 81–92.

Kudyk M., Pilecki, Z. (2009). *Moduł deformacji utworów fliszu karpackiego na trasie tunelu Emilia w Beskidzie Żywieckim*. Zeszyty Naukowe IGSMiE PAN 76, 45–63.

Linowski, H. (1969). O zależności między dynamicznym a statycznym modułem sprężystości Younga. *Acta Geoph. Pol.*, 17, 1.

Łapczyński, M., Pilecki, Z., Krawiec, K., Słomian, A., Pilecka, E., Łątka, T. (2025). Modelling of P-wave velocity changes in coal seams with increased depth: a case study. *Sci Rep* 15, 3413. <https://doi.org/10.1038/s41598-025-87417-6>.

Majcherczyk, T., Pilecki, Z., Niedbalski, Z., Pilecka, E., Blajer, M., Pszonka, J. (2012). Wpływ warunków geologiczno-inżynierskich i geotechnicznych na dobór parametrów obudowy wstępnej tunelu drogowego w Lalikach. *Gospodarka Surowcami Mineralnymi/ Mineral Resources Management* 28(1), 103–124.

Marcak, H., Zuberek, W. (1994). *Geofizyka Górnictwa*. Katowice: Śląskie Wydawnictwo Techniczne.

McCann, D.M., Culshaw, M.G., & Northmore, K.J. (1990). Rock mass assessment from seismic measurements. In *Proceedings of the 24th Annual Conference of the Engineering Group of the Geological Society on Field Testing in Engineering Geology* (pp. 257–266). London.

Paterson, M.S., Wong, T.F. (2005). *Experimental Rock Deformation – The Brittle Field*, 2nd ed., Berlin, Heidelberg, and New York: Springer.

Peryt, T.M. (1978). Sedimentology and paleoecology of the Zechstein Limestone (Upper Permian) in the Fore-Sudetic area (western Poland). *Sedimentary Geology* 20, 217–243.

Pilecki, Z. (1999). Dynamic Analysis of Mining Tremor Impact on Excavation in Coal Mine. In *FLAC and Numerical Modeling in Geomechanics*; Detournay & Hart (eds) (pp. 397–400). Boca Raton, FL, USA: CRC Press.

Pilecki, Z. (2018). *Metoda sejsmiczna w geoinżynierii*. Kraków: Wydawnictwo IGSMiE PAN.

Pilecki, Z., Krawiec, K., Pilecka, E., Nagy, S., Łątka, T. (2025). Temperature anomaly as an indicator of groundwater flow prior to the shaft sinking with the use of artificial ground freezing. *Engineering Geology* 347, 107916. <https://doi.org/10.1016/j.enggeo.2025.107916>

Pilecki, Z., Laskowski, M., Hryciuk, A., Pilecka, E., Czarny, R., Wróbel, J., Koziarz, E., Krawiec, K. (2013). Identification of gaso-geodynamic zones in the structure of copper ore deposits using geophysical methods. *CIM Journal* 5(3), 194–202.

Reynolds, J. M. (2011). *An introduction to applied and environmental geophysics* (2nd ed.). Chichester: John Wiley & Sons Ltd.

Schneider, B. (1967). Contribution à l'étude de massifs de la fondations de barrages. *Transactions du Laboratoire de Géologie, Faculté des Sciences, Université de Grenoble* 7, 1054–1094.

Siggins, A. F. (1993). Dynamic elastic tests for rock engineering. In J. A. Hudson (Ed.), *Comprehensive rock engineering* (Vol. 3, pp. 601–618), Oxford: Pergamon Press.

Sjögren, B., Ofsthul, A., Sandberg, J. (1979). Seismic classification of rock mass qualities. *Geophysical Prospecting* 27, 409–442.

Sutherland, R.B. (1962). Some dynamic and static properties of rocks. In *Proceedings of the 5th Symposium on Rock Mechanics* (pp. 473–490). Minnesota.

Ślizowski, J., Pilecki, Z., Urbańczyk, K., Pilecka, E., Lankof, L., Czarny, R. (2013). High-energy interactions and geomechanical implications in rock mass behavior. *Advances in High Energy Physics*, Article ID 461764. <https://doi.org/10.1155/2013/461764>

Tajduś A., Cała M., Tajduś K. (2012). *Geomechanika w budownictwie podziemnym: projektowanie i budowa tuneli*. Wydawnictwa AGH. Kraków.